SIMULATION OF R-1234yf PERFORMANCE IN A TYPICAL AUTOMOTIVE SYSTEM

Claudio Zilio,[(a)] J. Steven Brown, [(b)(c)] and Alberto Cavallini[(a)]

[(a)]Dipartimento di Fisica Tecnica, Università di Padova, Padova, 35131, Italy
[(a)]Department of Mechanical Engineering, Catholic University of America, Washington, DC 20064 USA
[(c)]Corresponding author:
Department of Mechanical Engineering, Catholic University of America, 620 Michigan Ave, NE, Washington, DC 20064 USA
brownjs@cua.edu; fax:1-202-319-5173

ABSTRACT

Simulations are conducted using R-1234yf (2,3,3,3-tetrafluoropropene; $CF_3CF=CH_2$) in a typical baseline R-134a small-size European automotive air-conditioning system, where the baseline R-134a system has a nominal cooling capacity of 5.8 kW at a compressor volumetric flow rate of 7.8 $m^3\ h^{-1}$. If R-1234yf is used as a drop-in replacement in this baseline system, its cooling capacity is 2.0 % lower than the R-134a value, and its COP is 1.0 % lower than the R-134a value. If on the other hand, the two systems are compared at equal cooling capacities, the COP values of the R-1234yf system are 0 % to 4 % lower than the R-134a values over operating conditions from idle to highway speeds. While both systems would benefit from the use of a liquid-line/suction-line heat exchanger, R-1234yf would benefit somewhat more from its use than would R-134a. Also, R-1234yf could benefit from the optimization of the heat exchanger circuitries. The thermodynamic and transport properties of R-1234yf are estimated from Brown et al. (2009a). The simulation results and analyses presented in this paper demonstrate the attractiveness of R-1234yf as a potential replacement for R-134a in automotive applications.

1. INTRODUCTION

The European Union's f-gas regulations (Regulation (EC) No 842/2006 and Directive 2006/40/EC) specify that beginning on January 1, 2011 new models and on January 1, 2017 new vehicles fitted with air conditioning can not be manufactured with fluorinated greenhouse gases having global warming potentials (GWP) greater than 150. Recently, R-1234yf, which has a 100-year time horizon GWP of four relative to carbon dioxide (Nielsen et al. 2007) has been investigated (e.g., Spatz and Minor 2008) as a possible replacement fluid for R-134a in automotive applications. This paper uses thermodynamic and transport property estimates of R-1234yf (provided in an accompanying paper by Brown et al., 2009a) to simulate its potential performance capabilities in an automotive system. These results are compared with the baseline refrigerant R-134a.

2. IDEAL VAPOR COMPRESSION REFRIGERATION CYCLE PERFORMANCE

In order to gauge the performance potential of R-1234yf, this section compares R-134a and R-1234yf in an idealized vapor compression refrigeration cycle. The cycle chosen is meant to be representative of typical automotive operating conditions, and is specified by a constant evaporation temperature of 10 °C, a constant condensation temperature of 50 °C, an evaporator superheat of 5 °C, a condenser subcooling of 5 °C, and a compressor isentropic efficiency of 70 %.

A modified version of CYCLE_D Ver. 4.0 (Brown et al., 2009b) was used to perform the simulations, where REFPROP 8.0 (Lemmon et al., 2007) was used to determine the thermodynamic properties of R-134a and the thermodynamic properties of R-1234yf were taken from Brown et al. (2009a). In the case of R-134a, REFPROP implements the Equation of State of Tillner-Roth and Baehr (1994) and fluid-specific transport property formulations fitted to extensive experimental data.

Figure 1 presents the simulation results of R-134a and Figure 2 presents the simulation results of R-1234yf. The Coefficient of Performance (COP) of the R-134a cycle is 4.118 and that of the R-1234yf cycle is 3.973, that is, the R-134a COP is 3.6 % greater than the R-1234yf cycle. The Volumetric Cooling Capacity (VCC) of the R-134a cycle is 2858 kJ m^{-3} and that of the R-1234yf cycle is 2633 kJ m^{-3}, that is the R-134a VCC is 8.5 % greater than the R-1234yf value.

Several observations can be made. First, the compressor discharge temperature for R-134a is some 7 °C higher than the R-1234yf value, implying a larger superheat loss for R-134a and thus a lowering of its COP vis-à-vis R-1234yf. This is a direct result of the larger slope of the saturated vapor line for R-1234yf. Second, the compressor work for the two refrigerants is similar; whereas, the refrigeration capacity per mass is larger for R-134a, thus implying better COP for R-134a. Third, though not obvious from the figures, the expansion losses are larger for R-1234yf, implying a reduction in its COP and indicating that it would benefit more than R-134a from the use of a liquid-line/suction-line heat exchanger (LLSL-HX). For example, for the above described cycle, though with zero subcooling, the COP and VCC values for R-134a are 3.898 and 2705 kJ m^{-3}, respectively, and for R-1234yf are 3.700 and 2451 kJ m^{-3}, respectively. If the cycles are supplemented with LLSL-HXs with efficiency values of 75 %, the values for R-134a are 4.025 and 2821 kJ m^{-3}, respectively, and for R-1234yf are 3.953 and 2658 kJ m^{-3}, respectively. That is, the COP and VCC values for the R-134a cycle with a LLSL-HX are 3.3 % and 4.3 %, respectively, greater than the baseline R-134a cycle. On the other hand, the COP and VCC values for the R-1234yf cycle with a LLSL-HX are 6.8 % and 8.4 %, respectively, greater than the baseline R-1234yf cycle. Fourth, though not shown in the figures, the R-1234yf suction vapor is some 15 % denser than the R-134a value; however, the refrigeration capacity per mass of R-134a is some 25 % greater than the R-1234yf value, leading to the better VCC for R-134a.

In the next section, a more complete simulation model capable of capturing non-ideal effects, e.g., exergy losses in the heat exchangers, is used to simulate the performance potentials of R-134a and R-1234yf in a typical automotive system.

3. "REAL" VAPOR COMPRESSION REFRIGERATION CYCLE PERFORMANCE

The simulation model used is described in detail in Casson et al. (2003), and thus will only be discussed briefly here. It consists of a compressor model (either defined by a compressor map or by isentropic and volumetric efficiencies), a tube-fin evaporator model, and either a tube-fin condenser model or a mini-channel condenser model. For calculation purposes, the heat exchangers are divided into a series of small three-dimensional cells. The refrigerant-side heat transfer, pressure drop, and void fraction correlations are listed in Table 1. The air-side heat transfer coefficients are assumed to be uniform and given by constant values.

A simulation proceeds by iterating on the evaporation and condensation pressures, ceasing when the model successfully matches the refrigerant mass flow rate of the compressor to those in the evaporator and condenser.

A typical small-size R-134a-based European automotive air conditioning system with a nominal cooling capacity of 5.8 kW at a compressor volumetric flow rate ($\dot{V}$) of 7.8 m^3 h^{-1} is considered. The system consists of a mini-channel evaporator, a mini-channel condenser, a compressor, and a thermostatic expansion device. In order to use the existing simulation model (which consists of a tube-fin evaporator

model), a tube-fin evaporator was designed to match the performance curve provided by the manufacturer of the mini-channel evaporator. The geometrical characteristics of the evaporator and the condenser are provided in Table 2. For the purposes of this paper, the compressor is defined by a constant isentropic efficiency of 70 % and a constant volumetric efficiency of 100 %. The thermostatic expansion device establishes the refrigerant mass flow to be the value determined by the iteration process described previously.

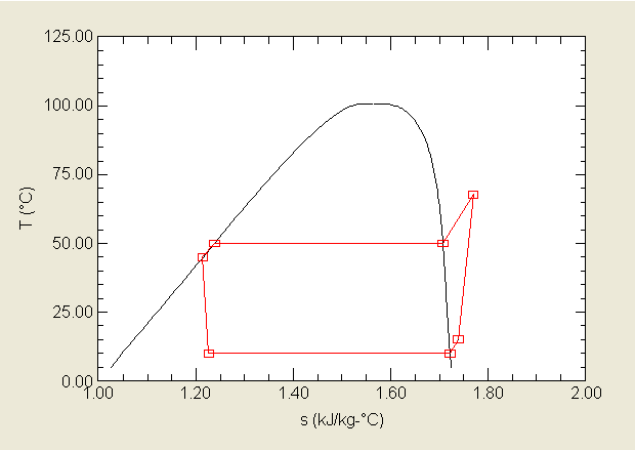

Figure 1a. *T-s* State Diagram for R-134a.

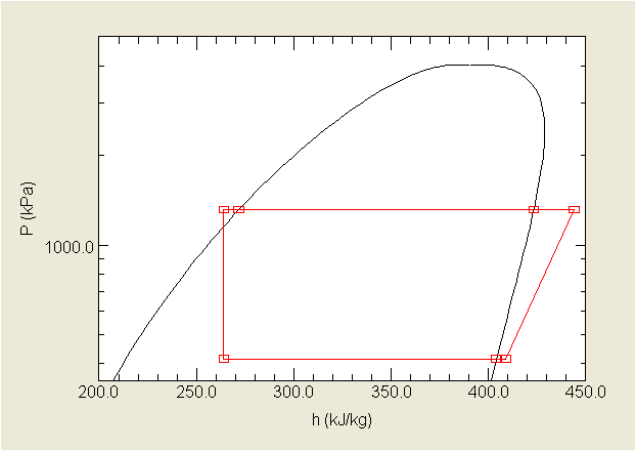

Figure 1b. *P-h* State Diagram for R-134a.

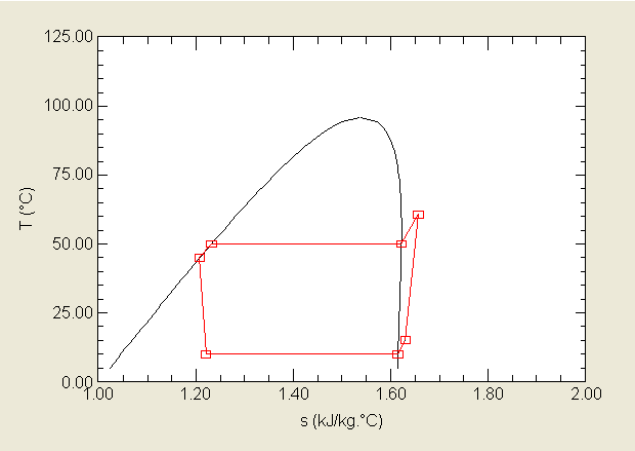

Figure 2a. *T-s* State Diagram for R-1234yf.

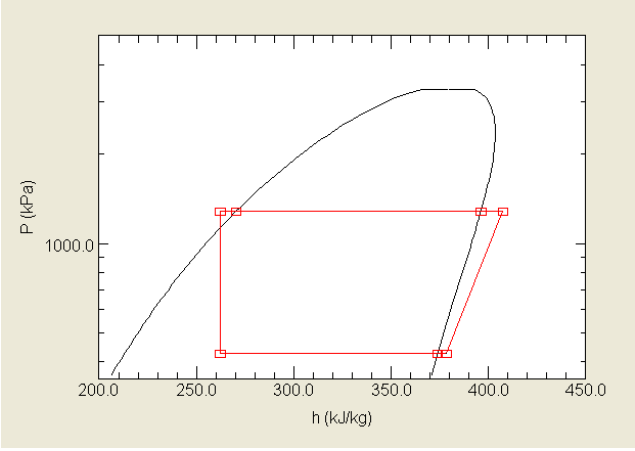

Figure 2a. *P-h* State Diagram for R-1234yf.

Table 1. Correlations used for the evaporator and the condenser.

Refrigerant-side heat transfer coefficient for the evaporator	Kattan et al. (1998)
Refrigerant-side heat transfer coefficient for the condenser	Cavallini et al. (2006)
Refrigerant-side pressure drop for the evaporator	Friedel (1979)
Refrigerant-side pressure drop for the condenser	Cavallini et al. (2006)
Refrigerant void fraction	Rouhani and Axelsson (1970)
U-bend pressure drop	Equivalent length = 30*D*
Air-side heat transfer coefficient for the evaporator	Manufacturer supplied data
Air-side heat transfer coefficient for the condenser	Chang & Wang (1997)

Table 2. Geometrical description of the mini-channel condenser and the micro-fin tube evaporator.

Micro-fin tube evaporator		Mini-channel condenser	
Longitudinal tube spacing[1]	12.7 mm	Width of flattened tube	16.51 mm
Transverse tube spacing[2]	21.0 mm	Height of flattened tube	1.65 mm
Tube length	250 mm	Length of flattened tube	630 mm
Inside tube diameter	6.95 mm	Spacing between flattened tubes	10.54 mm
Number of rows	4	Number of flattened tubes	44
Number of tubes per row	12	Number of refrigerant passes	2
Number of refrigerant circuits	6	Number of flattened tubes/pass	36/8
Fin spacing	1.8 mm	# of minichannels/flattened tube	13
Fin thickness	0.11 mm	Minichannel diameter	0.787 mm
Simulation elements per tube	10	Fin spacing	1.2 mm
Ratio of external to internal area	12.1	Fin height	8.9 mm
		Fin length	16.51
		Fin thickness	0.1 mm
		Simulation elements/flattened tube	20
		Ratio of external to internal area	8.67

[1]parallel to air flow [2]normal to air flow

The operating conditions are typical of those for an automotive system and are provided in Table 3. Note: the condenser subcooling values were found by performing a series of simulations where the subcooling values were incrementally increased from zero. The subcooling values used in the remaining simulations (and reported in Table 3) are the ones that maximized the COP values.

Table 3. Operating conditions.

Micro-fin tube evaporator		Mini-channel condenser	
Superheat	5.0 °C	Subcooling	5.0 °C (R-134a) 7.0 °C (R-1234yf)
Inlet air temperature	35.0 °C	Inlet air temperature	35.0 °C
Inlet air relative humidity	60.0 %	Volumetric flow rate of air	3150 m^3 h^{-1}
Mass flow rate of air	500 kg h^{-1}	Face velocity of air	3.0 m s^{-1}
Face air velocity	4.0 m s^{-1}	Air-side heat transfer coefficient[1]	142 W m^{-2} K^{-1}
Air-side heat transfer coefficient[1]	115 W m^{-2} K^{-1}		

[1]Effective value, inclusive of fin efficiency

4. SIMULATION RESULTS FOR A "REAL" CYCLE

4.1 Performance with Constant Compressor Volumetric Capacity

Table 4 provides simulation results for R-134a and R-1234yf for a constant compressor $\dot{V}$ of 7.8 m^3 h^{-1}, that is, they represent a drop-in replacement of R-134a with R-1234yf. Several interesting observations can be made. First, the compressor discharge temperature for R-1234yf is approximately 6.0 °C less than the R-134a value. Second, the cooling capacity for R-1234yf is 2.0 % less than the R-134a value. Third, the COP for R-1234yf is 1.0 % less than the R-134a value. Fourth, $\dot{m}_{ref}$ for R-1234yf is some 20 % greater than the R-134a value due to the denser suction vapor of R-1234yf. Fifth, the evaporation temperature of the R-1234yf system is 0.51 °C greater than the R-134a value, and the condensation temperatures of the R-1234yf system is 0.19 °C greater than the R-134a system. Despite these differences, the results confirm the attractiveness of R-1234yf as a potential replacement for R-134a in automotive applications. In the next sections, simulation results will be presented first for constant cooling capacity and then secondly for equal COP values.

Table 4. R-134a and R-1234yf simulation results for constant compressor $\dot{V}$ of 7.8 $m^3\ h^{-1}$.

	$\dot{m}_{ref}$ (kg h^{-1})	Q_{evap} (W)	T_{evap} (°C)	T_{disch} (°C)	Q_{cond} (W)	T_{cond} (°C)	COP
R-134a	144.1	5832	9.66	67.47	7253	50.33	4.06
R-1234yf	173.1	5715	10.17	61.37	7141	50.52	4.02

4.2 Performance with Constant Cooling Capacity

The objective of this subsection is to compare the two systems at constant cooling capacities. The results are presented in Table 5, where the cooling capacity range was chosen to approximately cover compressor speeds from idle to highway driving. Several interesting observations can be made. First, the compressor discharge temperatures for R-1234yf are approximately 3.9 °C to 7.6 °C less than the R-134a values. Second, the COPs for R-1234yf are 0 % to 4.3 % lower than the R-134a values. Third, $\dot{m}_{ref}$ values for R-1234yf are some 20 % to 26 % greater than the R-134a values due to the denser suction vapor of R-1234yf. Fourth, the evaporation temperatures of the R-1234yf system are from 0.17 °C smaller to 0.41 °C greater than the R-134a values, while the condensation temperatures of the R-1234yf system are from 0.49 °C to 0.95 °C greater than the R-134a values.

Table 5. R-134a and R-1234yf simulation results for constant cooling capacities.

	$\dot{m}_{ref}$ (kg h^{-1})	Q_{evap} (W)	T_{evap} (°C)	T_{disch} (°C)	Q_{cond} (W)	T_{cond} (°C)	COP
R-134a	75.6	3364	16.85	57.63	3865	44.28	6.71
R-1234yf	92.1		17.20	53.78	3875	44.85	6.59
R-134a	100.3	4276	14.27	62.31	5102	46.48	5.44
R-1234yf	121.0		14.68	56.55	5061	46.97	5.44
R-134a	144.1	5832	9.66	67.47	7253	50.33	4.06
R-1234yf	178.3		9.72	61.80	7332	51.01	3.92
R-134a	162.4	6418	7.73	71.31	8170	51.84	3.65
R-1234yf	202.5		7.64	63.96	8268	52.68	3.49
R-134a	188.2	7202	4.83	74.63	9469	54.07	3.15
R-1234yf	237.2		4.66	66.99	9590	55.02	3.03

4.3 Performance for Equal COP Values

Finally, in this subsection, the two systems are compared at equal energy efficiencies, with the results being presented in Table 6. Several interesting observations can be made. First, the compressor discharge temperatures for R-1234yf are approximately 6.4 °C to 8.6 °C greater than the R-134a values. Second, the cooling capacities for R-1234yf are 1.1 % to 4.4 % lower than the R-134a values. Third, $\dot{m}_{ref}$ values for R-1234yf are some 14 % to 21 % greater than the R-134a values due to the denser suction vapor of R-1234yf. Fourth, the evaporation temperatures of the R-1234yf system are from 0.38 °C to 1.02 °C greater than the R-134a values, while the condensation temperatures of the R-1234yf system are from 0.03 °C to 0.41 °C greater than the R-134a values.

Table 6. R-134a and R-1234yf simulation results for equal COP values.

	$\dot{m}_{ref}$ (kg h^{-1})	Q_{evap} (W)	T_{evap} (°C)	T_{disch} (°C)	Q_{cond} (W)	T_{cond} (°C)	COP
R-134a	75.6	3364	16.85	57.63	3865	44.28	6.71
R-1234yf	86.5	3217	17.69	59.66	3654	44.46	
R-134a	100.3	4276	14.27	62.31	5102	46.48	5.44
R-1234yf	118.9	4230	14.85	62.73	4977	46.83	
R-134a	144.1	5832	9.66	67.47	7253	50.33	4.06
R-1234yf	174.6	5714	10.04	68.02	7178	50.74	
R-134a	162.4	6418	7.73	71.31	8170	51.84	3.65
R-1234yf	195.5	6237	8.24	70.60	7993	52.19	
R-134a	188.2	7202	4.83	74.63	9469	54.07	3.15
R-1234yf	223.3	6918	5.85	74.60	9075	54.10	

5. CONCLUSIONS

Simulations were conducted using R-1234yf in a typical baseline R-134a small-size European automotive air conditioning system, where the baseline R-134a system has a nominal cooling capacity of 5.8 kW at a compressor volumetric flow rate of 7.8 m^3 h^{-1}. If R-1234yf is used as a drop-in replacement in this baseline system, its cooling capacity is 2.0 % lower than the R-134a value, and its COP is 1.0 % lower than the R-134a value. If on the other hand, the two systems are compared at equal cooling capacities, the COP values of the R-1234yf system are 0 % to 4 % lower than the R-134a values over operating conditions from idle to highway speeds.

While the evaporation and condensation temperatures are somewhat different between the two systems, the largest temperature differences can be seen in the compressor discharge temperatures. If R-1234yf is used as a drop-in replacement in the baseline system, its compressor discharge temperature is 6.0 °C lower than the R-134a value. If on the other hand, the two systems are compared at equal cooling capacities, the compressor discharge values of the R-1234yf system are 4.9 °C to 7.6 °C lower than the R-134a values over operating conditions from idle to highway speeds. These lower compressor discharge temperatures should lead to greater compressor reliability for the R-1234yf system.

While both systems would benefit from the use of a liquid-line/suction-line heat exchanger, R-1234yf would benefit somewhat more from its use than would R-134a. Also, R-1234yf could benefit from the optimization of the heat exchanger circuitries.

The thermodynamic and transport properties of R-1234yf are estimated from Brown et al. (2009a).

The simulation results and analyses presented in this paper demonstrate the attractiveness of R-1234yf as a potential replacement for R-134a in automotive applications.

ACKNOWLEDGEMENTS

The authors thank Mr. Giuseppe Romano for his assistance with the simulations. J. Steven Brown expresses his appreciation to the Dipartimento di Fisica Tecnica of the Università di Padova for hosting him for a sabbatical stay during the 2008-2009 academic year.

NOMENCLATURE

COP	Coefficient of Performance	h	specific enthalpy (kJ kg^{-1})
$\dot{m}$	mass flow rate (kg h^{-1})	P	pressure (kPa)
Q	heat transfer rate (W)	T	temperature (°C)
s	specific entropy (kJ kg^{-1} K^{-1})	$\dot{V}$	volumetric flow rate (m^3 h^{-1})
VCC	Volumetric Cooling Capacity (kJ m^{-3})		

Subscripts

cond	condenser or condensation	disch	compressor discharge
evap	evaporator or evaporation	ref	refrigerant

REFERENCES

Brown, J.S., Zilio, C., Cavallini, A., 2009a. Estimations of the thermodynamic and transport properties of R-1234yf using a cubic equation of state and group contribution methods. In: Proceedings of the 3rd IIR Conference on Thermophysical Properties and Transport Processes of Refrigerants, Boulder, CO, USA.

Brown, J.S., Domanski, P.A., Lemmon, E.W., 2009b. CYCLE_D Version 4.0: NIST vapor compression cycle design program. In: Proceedings of the 3rd IIR Conference on Thermophysical Properties and Transport Processes of Refrigerants, Boulder, CO, USA.

Casson, V., Del Belin Peruffo, G., Fornasieri, E., Zilio, C., 2003. Energy efficiency of a household air conditioner using new HFC refrigerants. In: Proceedings of the 21st International Congress of Refrigeration, Washington, DC, USA.

Cavallini, A., Doretti, L., Matkovic, M., Rossetto, L., 2006. Update on condensation heat transfer and pressure drop inside minichannels. Heat Transfer Engineering 27(4): 74-87.

Chang, Y.-J., Wang, C.-C., 1997. A generalized heat transfer correlation for louver fin geometry. Int. J. Heat Mass Transfer 40(3): 533-544.

Directive 2006/40/EC of The European Parliament and of the Council of 17 May 2006 relating to emissions from air-conditioning systems in motor vehicles and amending Council Directive 70/156/EC, 2006. Official Journal of the European Union. Retrieved online at: http://eur-lex.europa.eu/LexUriServ/LexUriServ.do?uri=OJ:L:2006:161:0012:0018:EN:PDF, September 18, 2008.

Friedel, L., 1979. Improved friction pressure drop correlations for horizontal and vertical two-phase pipe flow. European Two-Phase Flow Group Meeting, Ispra, Paper E2.

Kattan, N., Thome, J.R., Favrat, D., 1998. Flow boiling in horizontal tubes: part 3- Development of a new heat transfer model based on flow pattern. J. Heat Transfer 120(1): 156-165.

Lemmon, E.W., Huber M.L., and McLinden, M.O., 2007. NIST reference fluid thermodynamic and transport properties-REFPROP. NIST standard reference database 23-Version 8.0.

Nielsen, O.J., Javadi, M.S., Sulback Andersen, M.P., Hurley, M.D., Wallington, T.J., and Singh, R. 2007. Atmospheric chemistry of $CF_3CF{=}CH_2$: Kinetics and mechanisms of gas-phase reactions with Cl atoms, OH radicals, and O_3. Chemical Physical Letters 439: 18-22.

Regulation (EC) No 842/2006 of The European Parliament and of the Council of 17 May 2006 on certain fluorinated greenhouse gases, 2006. Official Journal of the European Union. Retrieved at: http://eur-lex.europa.eu/LexUriServ/LexUriServ.do?uri=OJ:L:2006:161:0001:0011:EN:PDF, September 18, 2008.

Rouhani, S.Z. and Axelsson, E. 1970. Calculation of volume void fraction in the subcooled and quality region. Int. J. Heat Mass Transfer 13: 383-393.

Spatz, M. and Minor, B., 2008. HFO-1234yf low GWP refrigerant update. In: Proceedings of the International Refrigeration and Air Conditioning Conference at Purdue, West Lafayette, Indiana, USA. Presentation retrieved online at:
http://refrigerants.dupont.com/Suva/en_US/pdf/MAC_Purdue_HFO_1234yf.pdf, September 18, 2008.

Tillner-Roth, R. and Baehr, H.D., 1994. An international standard formulation of the thermodynamic properties of 1,1,1,2-tetrafluoroethane (HFC-134a) for temperatures from 170 K to 455 K at pressures up to 70 MPa. J. Phys. Chem. Ref. Data 23: 657-729.